



Patel, R., Weller, M.T., and Price, D.J. (2007) Topological ferrimagnetism and superparamagnetic-like behaviour in a disordered homometallic coordination network. *Dalton Transactions*, 2007 (36). pp. 4034-4039. ISSN 1477-9226

<http://eprints.gla.ac.uk/12272>

Deposited on: 3 October 2012

This is a post-print version of an article which was published by the Royal Society of Chemistry in the journal Dalton Transactions.

The published article can be found at:

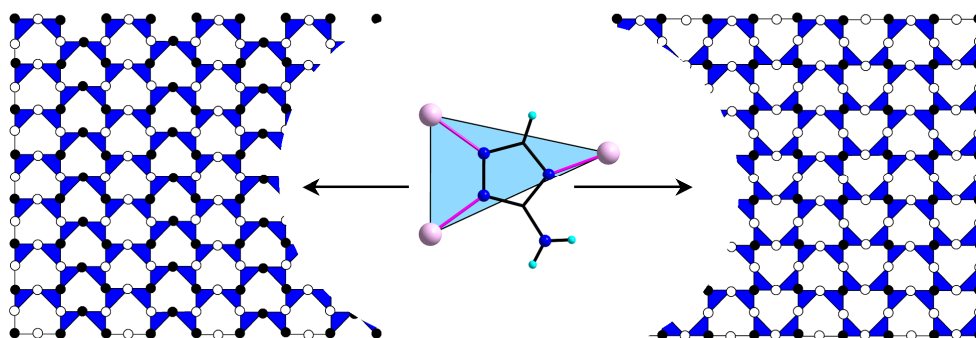
<http://pubs.rsc.org/en/Content/ArticleLanding/2007/DT/b706829h>

The article should be cited as:

R. Patel, D.J. Price and M.T. Weller, *Dalton Trans.*, 2007 (36), 4034-4039.

## Topological Ferrimagnetism and Superparamagnetic-like Behaviour in a Disordered Homometallic Coordination Network

Rina Patel, Mark T. Weller and Daniel J. Price\*



In this three dimensionally coupled cobalt(II) network, two dimensional disorder of the ligand orientation, results in novel magnetic phase behaviour at low temperatures.

# Topological Ferrimagnetism and Superparamagnetic-like Behaviour in a Disordered Homometallic Coordination Network†

Rina Patel,<sup>a</sup> Mark T. Weller<sup>a</sup> and Daniel J. Price<sup>\*b</sup>

<sup>a</sup> School of Chemistry, University of Southampton, University Road, Highfield, Southampton, SO17 1BJ, UK.

<sup>b</sup> WestCHEM, Department of Chemistry, University of Glasgow, University Avenue, Glasgow, G12 8QQ, UK. Fax: (+44)1413304888; E-mail: [D.Price@chem.gla.ac.uk](mailto:D.Price@chem.gla.ac.uk)

† Supporting information for this article is available on the WWW.

Crystals of a cobalt(II) 3-amino-1,2,4-triazolate;  $\text{Co}_2\text{Cl}(\text{C}_2\text{N}_4\text{H}_3)_3$ , **1** can be formed from a hydrothermal synthesis. X-ray crystallography shows an extended 3-dimensional network structure within a hexagonal space group with  $a = 9.9655(7)$  and  $c = 7.7523(7)$  Å. The data reveals an orientational disorder to the ligand. Structural considerations suggest that the ligand orientation is strongly correlated in 1-dimension, but the nature and length scale of the 2-dimensional order is not obvious. The structure is discussed in terms of three key structural models, two of which are crystallographically ordered, while the third is disordered in 2-dimensions. The effect of ligand orientation on the network topology has profound effects on the expected magnetic behaviour, with two of the fully ordered models having either antiferromagnetic or ferrimagnetically ordered ground states. The magnetism of **1** is complex. It shows an antiferromagnetically coupled paramagnetic phase above ~5.3 K. Below ~4.5 K we see a ferrimagnetically ordered state ( $H_{\text{coer}} = 50$  Oe,  $M_{\text{rem}} = 1830$  Oe cm<sup>3</sup> mol<sup>-1</sup>,  $M_{\text{sat}} = 3450$  Oe cm<sup>3</sup> mol<sup>-1</sup> at 2 K). In the intermediate temperature range 4.5 to 5.3 K we see unusual behaviour with evidence of rapid, low-energy relaxation of the magnetisation. The unusual relationship between the structure and the magnetism of **1** is discussed in detail.

## Introduction

The ability of azoles,<sup>[1]</sup> triazoles<sup>[2]</sup> and tetrazoles<sup>[3]</sup> to bridge transition metal ions is central to the recent increased interest in their coordination chemistry. From a structural perspective You *et al*<sup>[4]</sup> have recently prepared a beautiful “open framework” materials from cobalt(II) and imidazole, which display extensive polymorphism and a zeolitic character. While iron(II) triazole coordination polymers<sup>[5]</sup> have been of interest to magnetochemists since many of these compounds show spin-crossover behaviour with thermal-hysteresis effects. Here the spin-crossover can drive a structural phase transition as the covalently bridged network can transmit geometric changes between iron centres. It is perhaps surprising that despite much work in this area, crystallographic structural information is often difficult to obtain. A third point of interest is in the ability of these linkages to mediate magnetic

super-exchange interactions which in an extended network can result in magnetic ordering.<sup>[1, 3, 5]</sup>

We present here  $[\text{Co}_2\text{Cl}(\text{3-amino-1,2,4-triazole})_3]$  (**1**), a complex and intriguing magnetically coupled coordination network. The implications of the observed ferrimagnetic ordering are discussed in view of the effect of structural disorder on the network topology.

## Results and Discussion

Hydrothermal reaction of  $\text{CoCl}_2$  and 3-amino-1,2,4-triazole in a 1:2 molar ratio yields  $[\text{Co}_2\text{Cl}(\text{3-amino-1,2,4-triazole})_3]$  (**1**) as a monophasic product. Optical microscopy shows it to be comprised of small blue needle-shaped crystals with a strong blue-pink dichroism. A typical crystal was selected for X-ray structure determination and the bulk sample purity was confirmed by microanalysis and PXRD.

### *X-ray crystal structure*

Crystallizing in a primitive hexagonal cell (Table 1) a good structural model for **1** was obtained in the non-polar space group  $P6_3/mmc$  (#194), revealing an aesthetically pleasing 3-dimensional coordination network. Selected geometric parameters are given in Table 2. The  $/m$  symmetry in space group #194 results in an orientational disorder of the triazolite ligand and of the position and orientation of the chloride and tetrahedral cobalt ions (Fig. 1).

The framework is composed of linear  $[\text{Co}(\text{C}_2\text{N}_4\text{H}_3)_3]_n^{n-}$  chains (Fig. 2), in which neighbouring octahedrally coordinated metal ions are linked by three bridging triazolite ligands, a common motif for such compounds.<sup>[6]</sup> These chains run parallel to the  $c$ -axis and are arranged in a hexagonal fashion with a second type of  $\text{Co}^{\text{II}}$  ion linking three columns through the coordination of the third triazolite nitrogen. Similar coordination of all three triazolite ring nitrogens is known.<sup>[7]</sup> The fourth site of this tetrahedrally coordinated cation is occupied by chloride (similar to the coordination of  $\text{Zn}^{\text{II}}$  in  $\text{Zn}(\text{C}_2\text{N}_3\text{H}_2)\text{Cl}$ <sup>[8]</sup>). Thus the structure contains stacks of tetrahedrally coordinated Co ions (Fig. 2).

Steric considerations require a given stack of  $\text{CoN}_3\text{Cl}$  tetrahedra to be polar, with all Co–Cl bond vectors aligned in the same direction (Fig. 2). No steric requirement exists for the relative orientations of neighbouring stacks. Thus while we may expect correlated ligand orientations in 1-dimension, the nature of the 2-dimensional ligand orientation correlation is much less clear.

Two simple structurally ordered scenarios may be derived from the  $P6_3/mmc$  description: model A (Fig. 2a) - all polar stacks point in the same direction, such a structure is described in the polar space group  $P6_3mc$ , #186, and model B (Fig. 2b) - alternate columns have Co–Cl bonds pointing in opposite directions. This non-polar structure has the same cell parameters but would be described in the space group  $P\bar{3}m1$ , #164. In addition to these structurally ordered arrangements a degree of structural disorder in the orientation of neighbouring stacks can also be envisaged. Complete disorder at microscopic length scales yields model C (a random orientation of stack polarity), which is best described in space group used; that is #194. As expected for this type of order-disorder relationship, the space groups of the ordered

structures (#164, #186) are maximal non-isomorphic subgroups of order 2 of the space group (#194) of the disordered structure.

However the disorder observed by modelling the diffraction data in space group #194 could also result from a simple macroscopic twinning of the ordered models A or B. Attempts to model the diffraction data using both ordered and twinned models (with constraints) gave either unstable or unsatisfactory refinements, suggesting that the disorder in **1** is microscopic in origin and model C is the best structural description.

We note that in principle diffuse scattering studies should qualify our model and could quantify the extent of any disorder.

Although local orientational disorder of this ligand has been reported previously,<sup>[9]</sup> in this case stereo-kinetic considerations suggest that once a particular orientation for a Co<sup>II</sup> tetrahedron occurs, then that orientation is propagated along the stack as the crystal grows. This type of disorder allows the entire structure to be divided into structurally ordered domains. In fact the division can be equally well described in terms of polar (model A) domains or non-polar (model B) domains (Fig. 3). In the likely event of a biased distribution the average domain size of the polar division is inversely related to the size of the non-polar division, and the true structure will lie somewhere on the trajectory between models A, C and B (Fig. 3d).

## ***Magnetism***

Field cooled magnetization measurements (FCM:  $H = 100$  Oe) on **1** reveal a significant increase in sample magnetization below  $\sim 5.3$  K, typical of an ordered magnetic phase with a spontaneous net moment (Fig. 4a). Fitting  $\chi(T)$  at high  $T$  to Curie-Weiss law gives  $C = 2.99(1) \text{ cm}^3 \text{ mol}^{-1} \text{ K}$  (where  $\text{mol}^{-1}$  is per mole of Co<sup>II</sup> ions not per mole of formula unit) and  $\theta = -58.2(8)$  K. The Curie constant equates to an  $S = 3/2$  ground state for both  $O_h$  and  $T_d$  Co<sup>II</sup> ions with an average  $g$ -value of 2.31. The negative Weiss constant indicates a dominant antiferromagnetic exchange interaction. Measurements at  $H = 50$  and  $200$  Oe show a strong field dependence of the susceptibility in the low temperature regime and field independent behaviour above the transition temperature. The FCM and zero-field cooled magnetization (ZFCM) show similar behaviour with the onset of a significant moment below  $5.3(1)$  K, while the remnant magnetization (REM) curve decays rapidly almost reaching zero by  $\sim 4.5$  K then decreasing more slowly above this temperature (Fig. 4a). We note that the bifurcation in the FCM and ZFCM curves ( $4.5$  K) is significantly lower than the onset of magnetisation ( $5.3$  K). The bifurcation temperature specifically indicates a point below which there is a significant energy barrier to the re-orientation of magnetic domains (usually associated with an anisotropy energy). It appears that in **1**, there is an unusual region between  $\sim 4.5$  and  $\sim 5.3$  K where there is no significant energy barrier to domain reorientation. Variable frequency ac susceptibility measurements were performed in the vicinity of the magnetic phase transition (Fig. 5). The position of the peak (maximum) at  $3.5$  K in both the real and imaginary components is independent of frequency. It corresponds to a transition to a long-range ordered magnetic state with a net moment. We note an unusual feature between  $4$  and  $5.2$  K, consisting of overlapping maxima. The position of the maxima and the shape of this part of the imaginary susceptibility has a frequency dependence, *suggestive* of a 'blocking' temperature and superparamagnetic-like or spin glass-like behaviour.<sup>[10]</sup> It appears that **1** shows at least three magnetic phases: Above  $5.3(1)$  K is a normal paramagnetic state, between  $\sim 4$  and  $5.3(1)$  K is an intermediate state and below  $\sim 4$  K

we see the formation of a more conventional long-range ferrimagnetically ordered phase. Field dependent measurements at 2.0, 3.0 and 3.5 K all show a very rapid increase in  $M(H)$  on application of the smallest field; while at 4.0, 4.5, 4.75 and 5.0 K the initial increase in  $M(H)$  is not so great; and measurements at 5.5 and 6.0 K reveal characteristic paramagnetic behaviour. Hysteresis measurements at 2 K (Fig. 4b) supports the proposed ferrimagnetic order;  $H_{coer} = 50$  Oe,  $M_{rem} = 1830$  Oe cm<sup>3</sup> mol<sup>-1</sup>. We determine the saturation magnetization as 3450 Oe cm<sup>3</sup> mol<sup>-1</sup> (per Co ion), corresponding to 18 % of the moment expected for a ferromagnetically aligned sample (using the average  $g$ -value determined from the high  $T$  susceptibility). The area enclosed by the hysteresis curve (work done on the sample) is 83.3 mJ mol<sup>-1</sup>. A similar measurement at 4.5 K shows virtually no remnant magnetization or coercivity, consistent with a fast (low-energy) relaxation process.

### ***Magnetostructural correlations***

Structural considerations are key to understanding the magnetism of **1**. There are three triazolate-mediated superexchange interactions (Fig. 1);  $J_1$  links  $O_h$  Co ions ( $d_{(Co...Co)} = 3.876$  Å) into chains along the  $c$ -axis,  $J_2$  and  $J_3$  both link a  $T_d$  ion to an  $O_h$  ion ( $d_{(Co...Co)} = 5.886$  and  $6.329$  Å). From previous studies<sup>[4b, 11]</sup> we expect antiferromagnetic interactions with  $J_1 \sim -12$  cm<sup>-1</sup> and  $J_2 \sim J_3 \sim -2$  cm<sup>-1</sup>. The 3-D magnetic order is a result of the interchain couplings  $J_2, J_3$ .<sup>[12]</sup> In the 3-D structure only two coupling interactions are required to connect all cobalt ions. These are either  $J_1$  and  $J_2$  or  $J_1$  and  $J_3$ . The scalene nature of the triangular plaquette formed by  $J_1, J_2$  and  $J_3$  (from a single bridging triazolate) means it is unlikely that any pair or couplings have equal magnitude. If we assume this to be the case, the weakest interaction ( $J_3$ ) can be neglected and we can arrange all spin moments connected by the strongest couplings ( $J_1, J_2$ ) with an antiparallel relationship. In this case all pairwise interactions are satisfied. Note that qualitatively the same results are obtained if  $J_2$  is the weakest interaction. However, the exact nature of the physical structure of **1** is crucial to the overall magnetic ground state. For both the polar model A and the non-polar model B we predict an ordered magnetic structure where Co<sup>II</sup>( $O_h$ ), ions linked by  $J_1$  have alternate spin polarization, while all Co<sup>II</sup>( $T_d$ ) ions in given stack have the same spin polarization. However, while for model A we expect neighbouring stacks to have opposite spin polarizations (Fig. 6 and 7a), resulting in an overall antiferromagnetic state, for the ordered non-polar structure (model B) we expect topological ferrimagnetic order<sup>[13]</sup> with all the Co<sup>II</sup>( $T_d$ ) stacks having the same spin alignment (Fig. 6 and 7b). Such a structure would have a saturation magnetization of  $\sim 8380$  Oe cm<sup>3</sup> mol<sup>-1</sup> (per Co ion; assuming  $g=2$  for Co<sup>II</sup>( $T_d$ )). The observed magnetization corresponds to 41 % of the expected value for the ferrimagnetic model (based on structural model B).

The effect of structural disorder on the ground state of **1** is quite unusual, the disorder of model C does not result in competing interactions and simple spin-glass behaviour is not expected. In fact, in the disordered model all  $J_1$  and  $J_2$  pairwise interactions can be satisfied, resulting in ferrimagnetic domains that can be mapped directly on the two domains for the non-polar ordered structure (Fig. 3f). Alternatively the space can be divided into ordered antiferromagnetic domains that can be mapped onto the structurally polar domains (Fig. 3e).

While the structurally ordered models should exhibit straight-forward behaviour (model A - antiferromagnet; model B - "topological" ferrimagnet) the observed

magnetic behaviour is evidence for a more disordered model C-like structure. We note that the magnetic ordering temperatures for models A and B should be slightly different, and that it is likely that structural domain size can influence  $T_c$ . It is well known that when particle size limits domain size materials can show superparamagnetic behaviour and characteristic blocking temperatures.

## Conclusions

In magnetic materials structural disorder is usually of the form of site or bond vacancies; the consequences of which are greatly dependent on the nature of the magnetic network. Clearly in 1-D materials a low level of such defects/impurities will have a huge impact on the maximum spin correlation length and the magnetic behaviour. Whereas in most 2 and 3-D structures such defects are less important, (as long as the defect concentration is well below the percolation threshold.)<sup>[14]</sup> The importance of spin frustration in a particular structure is also important, in highly frustrated systems defects can locally pin a particular magnetic structure,<sup>[15]</sup> thus increasing the ordering transition temperature, while it is more generally the case that defects result in competing interactions reducing transition temperatures and introducing spin glass behaviour.<sup>[10c]</sup>

In this case the orientational disorder of the ligand serves to fundamentally change the topology of the network. We can view the disorder as linking two ordered models; in model A there is a preference for parallel stack polarity, while in model B there is a preference for antiparallel stack polarity. The topology of these models support fundamentally different ground states; either antiferromagnetic order or ferrimagnetic order.<sup>[16]</sup>

In combination the structural data and the magnetic studies all point to a structural model with 1-D order and 2-D orientational disorder. Magnetically the unique structure permits an unusual and distinct intermediate magnetic phase, with little anisotropy and rapid dynamical processes. This material is clearly in need of much further study and both structural and magnetic experiments are planned to better qualify and quantify the interplay of structural disorder and magnetic order.

## Experimental

All reagents had a minimum 99% purity, and were used as received without further purification. Hydrothermal reactions were performed in 23 ml capacity Parr Teflon lined acid digestion bomb, model 4749. CHN analysis was obtained using a EAI Exeter Analytical Inc. CE-440 Elemental Analyzer. Cl analysis was determined by mercury titration. Infrared spectra were obtained on a Perkin Elmer Spectrum One FTIR spectrometer as pressed KBr pellets. UV/VIS/NIR spectra were recorded on a Perkin Elmer Lambda 19 spectrometer in diffuse reflectance mode using an anhydrous BaSO<sub>4</sub> matrix. Powder X-ray diffraction on a 12 mg sample of **1** was measured using a Siemens D5000 diffractometer with Cu K $\alpha$ 1 radiation ( $\lambda = 1.54 \text{ \AA}$ ) in the range  $5 < 2\theta < 75^\circ$ .

Magnetisation measurements were made on a Quantum Design MPMS SQUID magnetometer in both DC and RSO transport modes, on powdered samples held in an ecosane matrix to prevent reorientation effects. A diamagnetic correction of  $-52.65 \times$

$10^{-6} \text{ cm}^3 \text{ mol}^{-1}$  was determined from Pascal's constants.<sup>[17]</sup> Static (dc) measurements were performed between 2 - 290 K in several applied fields using FCM, ZFCM and REM protocols. Initial magnetisation curves were recorded between 0 and 50 kOe for a range of temperature in the vicinity of the low temperature ordered state. Full hysteresis measurements were recorded at selected temperatures between  $\pm 50$  kOe. Dynamic (ac) susceptibility measurements were performed between 2 - 6 K in zero offset field with a driving field of 3.5 Oe, for a range of frequencies between 20 and 1300 Hz.

Single crystal X-ray data was collected with Mo-K $\alpha$ 1 radiation (0.71073 Å) on an Enraf Nonius KappaCCD area detector as  $\phi$  and  $\omega$  scans to fill Ewald sphere. Data collection and cell refinement were managed by DENZO,<sup>[18]</sup> structure solution and refinement by SHELXS97<sup>[19]</sup> and SHELXL97<sup>[20]</sup> in the WinGX environment.<sup>[21]</sup> Crystallographic parameters are given in Tables 1 and 2. Crystallographic data for the structures has been deposited with the Cambridge Crystallographic Data Centre as supplementary publication CCDC 297715 (**1**). Note on the refinement of disorder: In the structure, the ligand is disordered over two orientations. Strictly the ligand has  $C_s$  symmetry, and the atomic coordinates for the ligand atoms need not be coincident. However, the near  $C_{2v}$  symmetry of the five ring atoms means that the coordinates of the ring atoms for the two orientations are very close. In fact we only see single peaks in the Fourier difference maps and no evidence of split peaks, as might be expected. These limits on the data quality meant that we choose to take a simplistic approach to the model, and constrained the ring atoms to an exact  $C_{2v}$  symmetry, with atomic coordinates for atoms from molecules with different orientations constrained to be the same. This approximation avoids the meaningless refinement of over correlated parameters. Better quality X-ray diffraction data or neutron diffraction experiments would allow a more realistic model. The consequence of our approach is that evidence of non-coincident atoms may be seen as prolate thermal parameters. We note that the ring atom N2 is markedly prolate, and it is our view that this “thermal parameter” has a significant component due to static structural disorder.

<Tables 1 and 2 here>

## Synthesis

*Catena-((tris( $\mu^3$ -3-amino-1,2,4-triazolato- $N^1, N^2, N^4$ ))-chloro dicobalt(II))* **1**: A mixture of  $\text{CoCl}_2 \cdot 6\text{H}_2\text{O}$  (100 mg, 0.42 mmol) and 3-amino-1,2,4-triazole (70 mg, 0.84 mmol) in distilled water (10 mL) was heated in a 23 ml capacity autoclave to 180 °C under autogenous pressure for 72 h before being cooled to room temperature. Blue needle-shaped crystals of  $\text{Co}_2\text{Cl}(\text{C}_2\text{N}_4\text{H}_3)_3$  (**1**) were collected by filtration, washed with distilled water and dried. Found C 17.68, H 2.19, N 40.00 (outside normal instrument range), Cl 8.37 %:  $\text{Co}_2\text{ClC}_6\text{H}_9\text{N}_{12}$  requires C 17.90, H 2.25, N 41.76, Cl 8.81%. Vibrational spectra (KBr)  $\bar{\nu}_{\text{max}}$  3419 (s), 3332 (s), 3141 (m), 2929 (w), 2804 (w), 2703 (w), 2592 (vw), 2483 (w), 2426 (w), 2255 (w), 2094 (vw), 1759 (m), 1614 (s), 1522 (vs), 1426 (s), 1384 (s), 1326 (w), 1282 (s), 1211 (s), 1132 (w), 1094 (m), 1047 (s), 1007 (m), 884 (m), 763 (s), 735 (m), 665 (s), 480 (s)  $\text{cm}^{-1}$ ; Electronic spectra  $\lambda/\text{nm}$  (abs/rel) 320 (0.6), 520 (0.38) ( $\text{Co}(\text{O}_h)$ ):  $\rightarrow {}^4\text{T}_{1g}(\text{P})$ , 620 (0.58) ( $\text{Co}(\text{T}_d)$ ):

→  ${}^4T_1(P)$ ), 1150 (0.55) (Co( $T_d$ ): →  ${}^4T_2(F)$ ), 1290 (0.58) (Co( $O_h$ ): →  ${}^4T_{2g}(F)$ ). PXRD,  $d/\text{Å}$  ( $k$ -vector), 8.4900 ( $1\bar{1}0$ ), 5.6917 ( $01\bar{1}$ ), 4.9377 ( $2\bar{1}0$ ), 4.2819 ( $2\bar{2}0$ ), 3.7509 ( $02\bar{1}$ ), 2.9948 ( $3\bar{2}1$ ), 2.8713 ( $3\bar{3}0$ ), 2.4886 ( $4\bar{2}0$ ), 2.0332, 1.8832, 1.7619, 1.6632, 1.3844.

## Acknowledgments

This work was supported by the EPSRC of the UK through grant GR/A00836/02. We thank Dr. H.J. Blythe (Sheffield University) for initial magnetic measurements, Dr. A. Parkin (Glasgow University) and Dr. M.E. Light (Southampton University) for helpful crystallographic discussions. We are also grateful to those referees who have provided constructive criticism.

## Notes and References

- [1] a) B.O. Patrick, W.M. Reiff, V. Sánchez, A. Storr, R.C. Thompson, *Inorg. Chem.*, **2004**, *43*, 2330; b) V. Sánchez, A. Storr, R.C. Thompson, *Can. J. Chem.*, **2002**, *80*, 133; c) S.J. Rettig, V. Sánchez, A. Storr, R.C. Thompson, J. Trotter, *J. Chem. Soc., Dalton Trans.*, **2000**, 3931; d) S.J. Rettig, A. Storr, D.A. Summers, R.C. Thompson, J. Trotter, *J. Am. Chem. Soc.*, **1997**, *119*, 8675.
- [2] a) J.G. Haasnoot, *Coord. Chem. Rev.*, **2000**, *200*, 131; b) S.J. Rettig, A. Storr, D.A. Summers, R.C. Thompson, J. Trotter, *Can. J. Chem.*, **1999**, *77*, 425.
- [3] A. Rodríguez, R. Kivekäs, E. Colacio, *Chem. Commun.*, **2005**, 5228.
- [4] a) Y.-Q. Tian, C.-X. Cai, Y. Ji, X.-Z. You, S.-M. Peng, G.-H. Lee, *Angew. Chem. Int. Ed.*, **2002**, *41*, 1384; b) Y.-Q. Tian, C.-X. Cai, X.-M. Ren, C.-Y. Duan, Y. Xu, S. Gao, X.-Z. You, *Chem. Eur. J.*, **2003**, *9*, 5673.
- [5] a) O. Kahn, C. Jay Martinez, *Science*, **1998**, *279*, 44; b) Y. Garcia, J. Moscovici, A. Michalowicz, V. Ksenofontov, G. Levchenko, G. Bravic, D. Chasseau, P. Gütllich, *Chem. Euro. J.*, **2002**, *8*, 4992.
- [6] a) Y. Garcia, P.J. van Koningsbruggen, G. Bravic, D. Chasseau, O. Kahn, *Eur. J. Inorg. Chem.*, **2003**, 356; b) Y. Garcia, P.J. van Koningsbruggen, G. Bravic, P. Guionneau, D. Chasseau, G. L. Cascarano, J. Moscovici, K. Lambert, A. Michalowicz, O. Kahn, *Inorg. Chem.*, **1997**, *36*, 6357; c) L. Antolini, A.C. Fabretti, D. Gatteschi, A. Giusti, R. Sessoli, *Inorg. Chem.*, **1991**, *30*, 4858; d) K. Drabent, Z. Ciunik, *Chem. Commun.*, **2001**, 1254; e) D. W. Engelfriet, G.C. Verschoor, W. Den Brinker, *Acta Cryst.*, **1980**, *B36*, 1554.
- [7] a) D.J. Chesnut, A. Kusnetzow, R. Birge, J. Zubieta, *Inorg. Chem.*, **1999**, *38*, 5484; b) J.-P. Zhang, S.-L. Zheng, X.-C. Huang, X.-M. Chen, *Angew. Chem. Int. Ed.*, **2004**, *43*, 206.
- [8] J. Krober, I. Bkouche-Waksman, C. Pascard, M. Thomann, O. Kahn, *Inorg. Chim. Acta*, **1995**, *230*, 159.
- [9] C.-Y. Su, A.M. Goforth, M.D. Smith, P.J. Pellechia, H.-C. zur Loye, *J. Am. Chem. Soc.*, **2004**, *126*, 3576.
- [10] See for example a) D.L. Leslie-Pelecky, R.D. Rieke, *Chem. Mater.* **1996**, *8*, 1770; b) I.J. Ortega, R. S. Puche, J. Romero de Paz, J.L. Martínez, *J. Mater. Chem.*, **1999**, *9*, 525; c) J.A. Mydosh, *Spin Glasses: An Experimental Introduction*, Taylor and Francis, (London) 1993.

- [11] a) L.R. Groeneveld, R.A. Le Fêbre, R.A.G. De Graaff, J.G. Haasnoot, G. Vos, J. Reedijk, *Inorg. Chim. Acta*, **1985**, *102*, 69; b) W. Vreugdenhil, J.G. Haasnoot, M.F.J. Schoondergang, J. Reedijk, *Inorg. Chim. Acta*, **1987**, *130*, 235.
- [12] The quoted coupling constants are defined from the pair-wise (or equivalent) Hamiltonian:  $\hat{H} = -2JS_1 \cdot S_2$ .
- [13] a) A.K. Ghosh, D. Ghoshal, E. Zangrando, J. Ribas, N.R. Chaudhuri, *Inorg. Chem.*, **2005**, *44*, 1786; b) E.-Q. Gao, Y.-F. Tue, S.-Q. Bai, Z. He, C.-H. Yan, *J. Am. Chem. Soc.*, **2004**, *126*, 1419; c) S. Konar, P.S. Munkherjee, E. Zangrando, F. Lloret, N.R. Chaudhuri, *Angew. Chem. Int. Ed.*, **2002**, *41*, 1561; d) N. Guillou, S. Pastre, C. Livage, G. Férey, *Chem. Commun.*, **2002**, 2358; e) M.A.M. Abu-Youssef, M. Drillon, A. Escuer, M.A.S. Goher, F.A. Mautner, R. Vicente, *Inorg. Chem.*, **2000**, *39*, 5022.
- [14] L.J. de Jongh, A.R. Miedema, *Adv. Phys.*, **2001**, *50*, 947.
- [15] W. Ratcliff II, S.-H. Lee, C. Broholm, S.-W. Cheong, Q. Huang, *Phys. Rev. B*, **2002**, *65*, 220406(R).
- [16] The phrase "topological" ferrimagnet is being increasingly widely used in this field. We would like to add a note of caution. The word "topological" is redundant in this phrase. Ferrimagnetism is always as a result of the topology of a magnetic network.
- [17] See for example: O. Kahn, *Molecular Magnetism*, VCH, Weinheim, **1993**.
- [18] Z. Otwinoski, W. Minor, in *Methods in Enzymology Vol. 276: Macromolecular Crystallography*, C. W. Carter Jr., R.M. Sweet, (eds), Academic Press, **1997**, part A, p. 307.
- [19] G. M. Sheldrick, *Acta Crystallogr.*, **1990**, *A46*, 467.
- [20] G. M. Sheldrick, University of Göttingen, Germany, **1997**.
- [21] L.J. Farrugia *J. Appl. Cryst.*, **1999**, *32*, 837.

## Figure captions

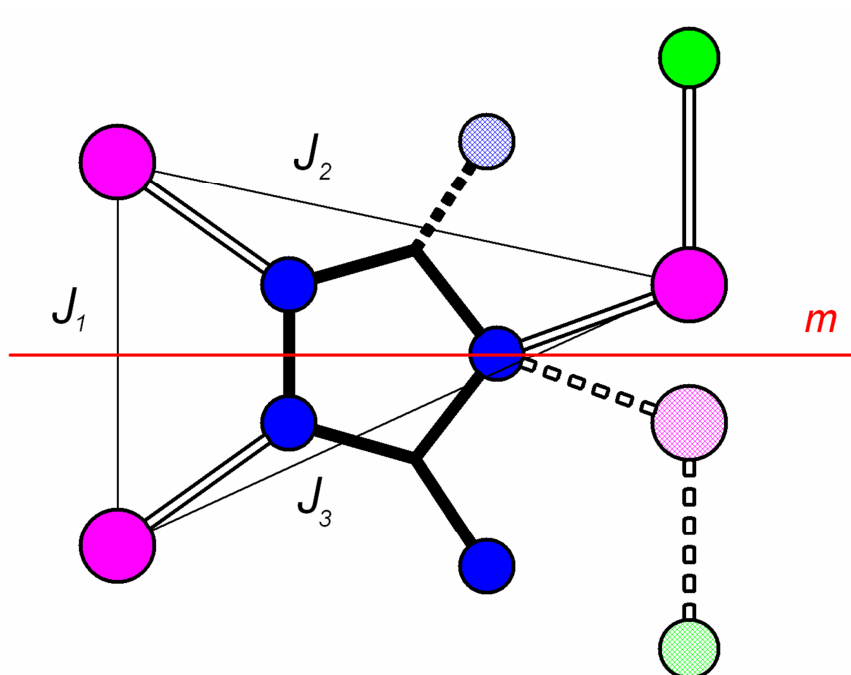


**Fig. 1** The coordination geometry of the ligand; Co - pink, Cl - green, N - blue, C - black. The mirror symmetry in space group #194 relates two possible ligand orientations. One orientation is shown with solid atoms and solid bonds. Cross-hatched atoms and dashed bonds are superimposed to show the second orientation. Note that the ligand orientation determines the orientation of the  $\text{CoN}_3\text{Cl}$  tetrahedron. Also shown are the triazolate mediated exchange coupled pathways for the first ligand orientation (solid atoms and bonds), as described in the text.

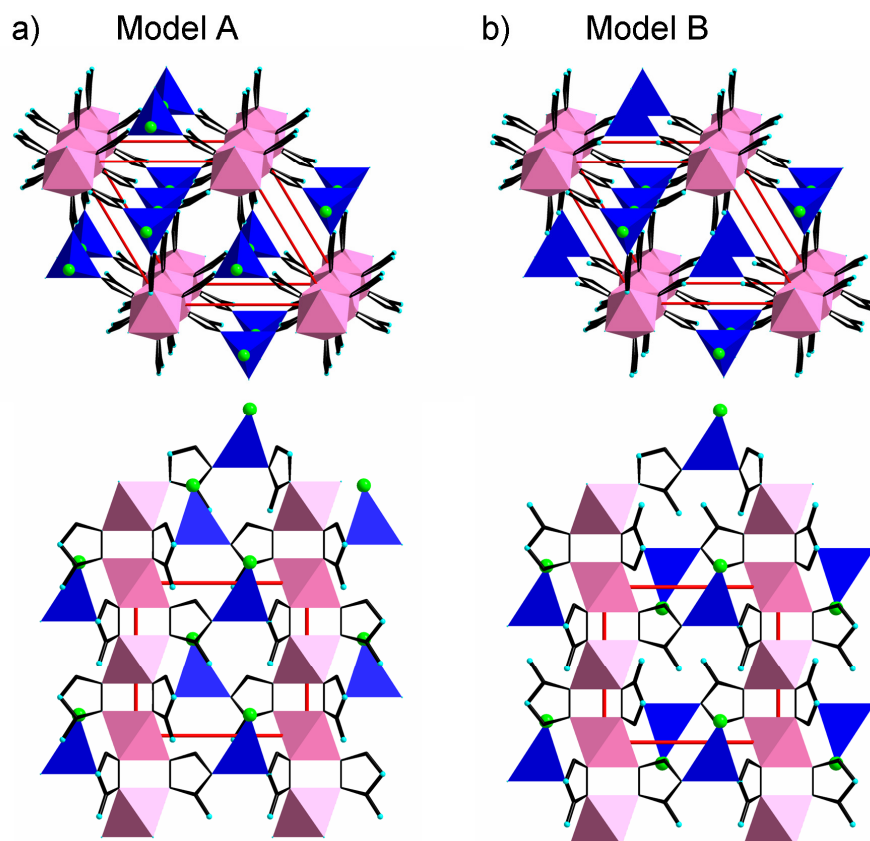


**Fig. 2** The network structure of **1**, showing how the triazolate ligand links Co ions (pink polyhedra – octahedral, blue polyhedra – tetrahedral) within structurally ordered portions. **a)** Structural model A; ordered with all the ligands having the same (down) orientation and all tetrahedra pointing upwards. **b)** Structural model B; with alternate stacks of tetrahedra having alternate up/down orientations (as defined by the Co-Cl bond vector).

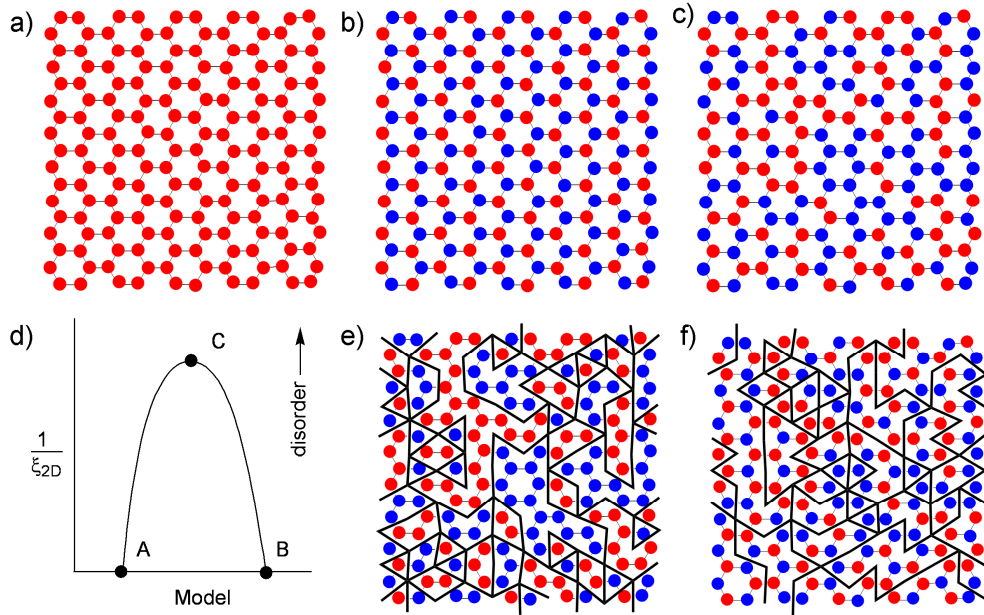


**Fig. 3** Schematic representation of the structural disorder in **1**. Viewed along the crystallographic  $c$ -axis, circles represent the stacks of  $\text{CoN}_3\text{Cl}$  coordination tetrahedra (blue,  $\text{Co-Cl}$  bond vector pointing upwards; red,  $\text{Co-Cl}$  bond vector pointing downwards). Not shown are the chains of octahedrally coordinated  $\{\text{CoN}_6\}$  Co ions which lie in the centres of the hexagons. **a)** Representation of the polar model A, as described in space group #186. **b)** Representation of the ordered non-polar model B as described by space group #164. **c)** Shows a random distribution of stack polarity, as described in the structural model C (*e.g.* space group #194). **d)** The qualitative relationship between the three models.  $\xi_{2D}$  is the 2-dimensional structural correlation length. The true structure of **1** is expected to lie on the curve that connects models A, B and C. **e)** Shows how the random structure can be divided into domains of alternate polarity - domains of structural model A (domain walls thick black lines) or **f)** equally well divided into domains with an antiparallel order - domains from structural model B. Note that between models, domain walls are spatially mutually exclusive. Magnetically ferrimagnetic domains are expected to map onto the non-polar structural domains of **f)** or antiferromagnetic domains can be mapped onto the polar structural domains shown in **e)**.

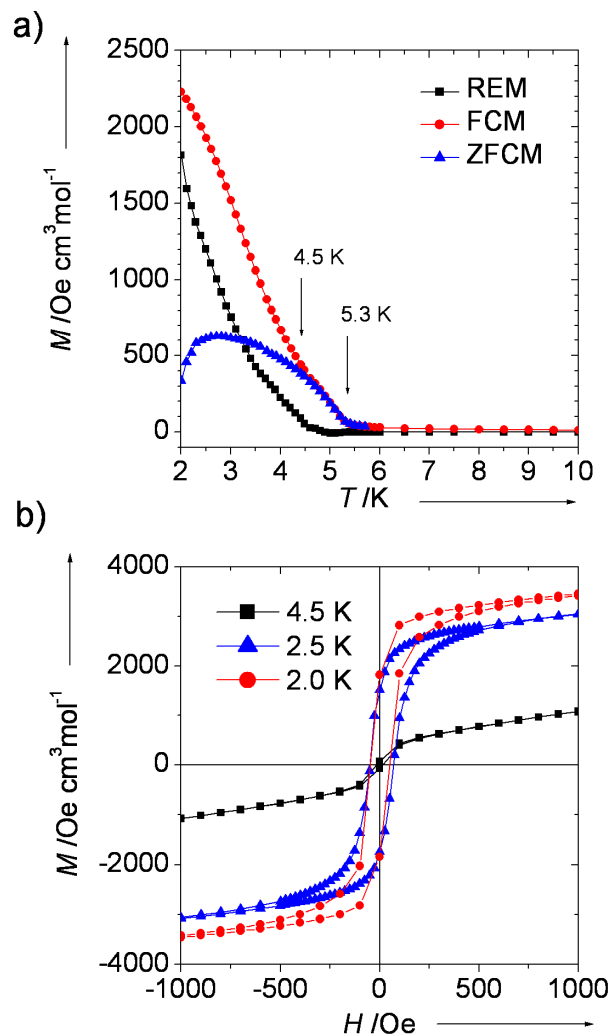


**Fig. 4** a) FCM ( $H_{\text{cooling}} = H_{\text{measure}} = 100$  Oe), ZFCM ( $H_{\text{cooling}} = 0$  Oe,  $H_{\text{measure}} = 100$  Oe) and REM ( $H_{\text{cooling}} = 100$  Oe,  $H_{\text{measure}} = 0$  Oe) measurements of **1**. b) Hysteresis measurements in both the low-temperature and intermediate magnetic phase.

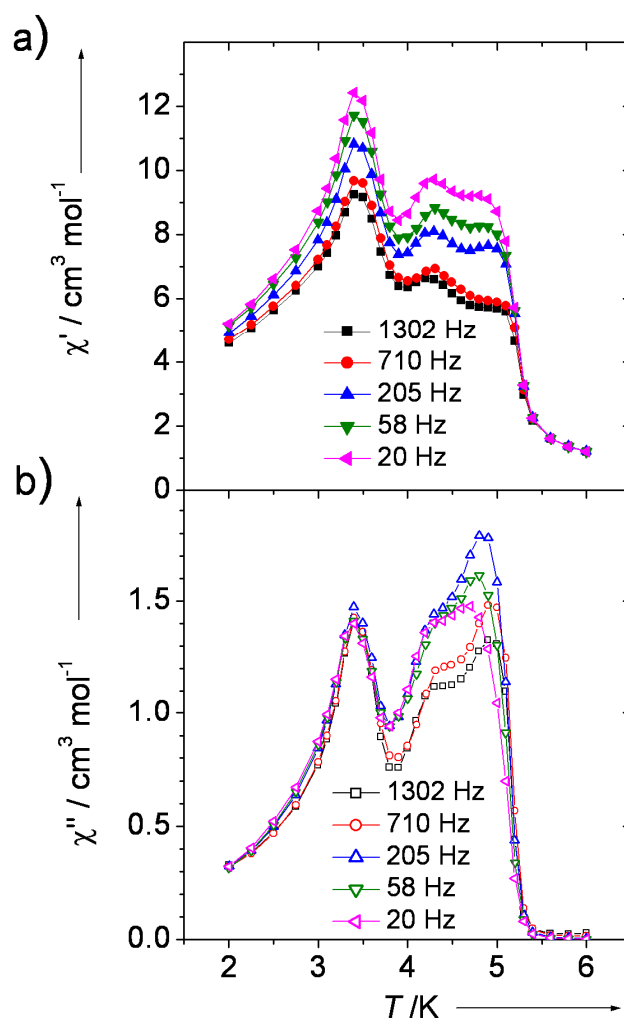


**Fig. 5** a) The real, in-phase component of the variable frequency ac susceptibility measurement and b) the imaginary, out-of-phase component.

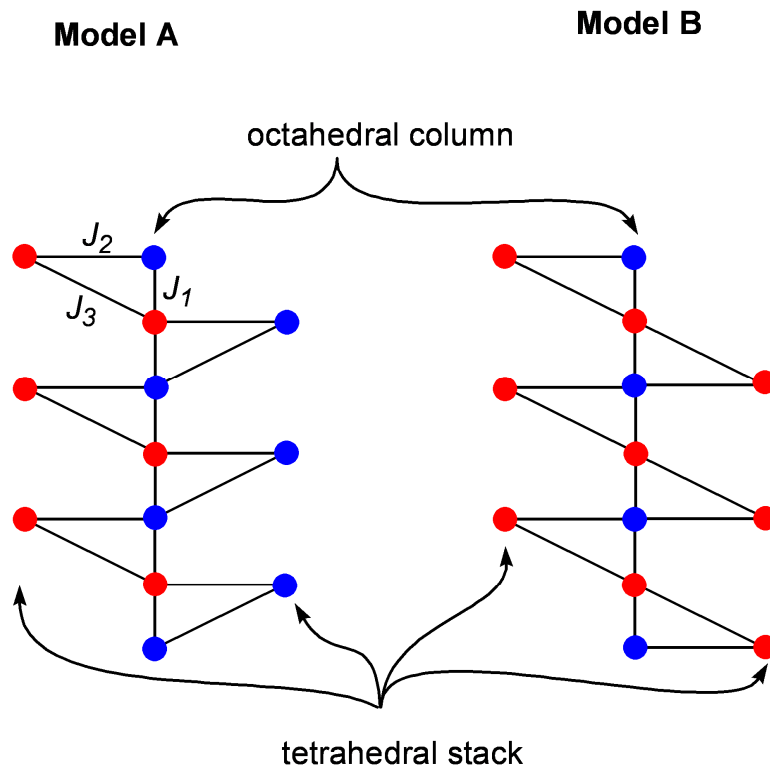


**Fig. 6** Schematic diagram showing the consequences of the alternate triazolate orientations, which result in qualitatively different magnetic ground states. Each triangle represents a bridging triazolate and the three magnetic couplings;  $J_1$  (vertical lines),  $J_2$  (horizontal lines),  $J_3$  (diagonal lines). If  $J_1$  and  $J_2$  mediate antiparallel spin alignments, then in model A half of all tetrahedral stacks have spin up (red circles) and the other half have spin down (blue circles), while in model B all tetrahedral ions have the same spin polarisation.

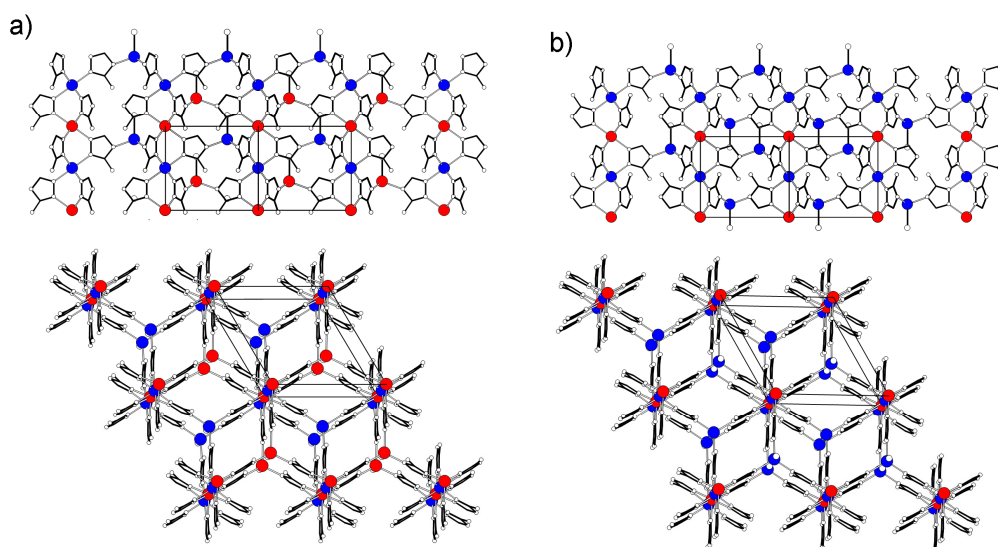


**Fig. 7** Extended magnetic models for **1**. Magnetic Co(II) ions are coloured; blue represents spin down, red represents spin up. **a)** Structural model A - all pairwise interactions ( $J_1$  and  $J_2$ ) are satisfied giving an antiferromagnetic ground state. **b)** Structural model B - with the same pairwise interactions ( $J_1$  and  $J_2$ ) satisfied gives a ferrimagnetic ground state.

**Table 1.** Crystal data for **1**.

Empirical formula	C <sub>6</sub> H <sub>9</sub> ClCo <sub>2</sub> N <sub>12</sub>
Formula weight	402.56 g mol <sup>-1</sup>
Crystal system	Hexagonal
Space group	<i>P</i> 6 <sub>3</sub> / <i>mmc</i>
<i>a</i>	9.9655(7) Å
<i>c</i>	7.7523(7) Å
<i>V</i>	666.74(9) Å <sup>3</sup>
<i>Z</i>	2
<i>T</i>	120 K
<i>D</i> <sub>calc</sub>	2.005 g cm <sup>-3</sup>
data/parameters	320/31
<i>R</i> 1 (all data/4σ( <i>I</i> ))	0.0904 / 0.0722
<i>wR</i> 2 (all data/4σ( <i>I</i> ))	0.1410 / 0.1357
Goodness-of-fit, <i>S</i>	1.257
Largest residual peak (hole)	0.592 (0.533) Å e <sup>-3</sup>
Data deposition reference	CCDC 297715

**Table 2.** Selected geometric parameters for **1**. Bond lengths /Å, bond angles /°.

N1—N1 <sup>i</sup>	1.393(10)	N1i—N1—C1	104.7(5)
N1—C1	1.317(10)	N1—C1—N2	114.1(8)
C1—N2	1.320(11)	C1—N2—C1 <sup>i</sup>	102.6(10)
C1—N3	1.337(14)	N1—C1—N3	136.9(10)
Co2—N2	2.049(10)	N2—Co2—C11	109.83(13)
Co2—C11	2.289(7)		
Co1—N1	2.126(6)		
Co1—Co1 <sup>i</sup>	3.876(1)	N1—Co1—N1 <sup>ii</sup>	180
Co1—Co2	5.887(1)	N1—Co1—N1 <sup>iii</sup>	89.3(2)
Co1 <sup>i</sup> —Co2	6.328(1)		

Symmetry operations: <sup>i</sup> = *y* - *x*, *y*, 1/2 - *z*; <sup>ii</sup> = *x* - *y*, -*y*, -*z*; <sup>iii</sup> = -*x*, *x* - *y*, *z*.